TURBULENCE EXCITED FREQUENCY DOMAIN DAMPING MEASUREMENT AND TRUNCATION EFFECTS

Jaak Soovere

Lockheed-California Company

SUMMARY

Existing frequency domain modal frequency and damping analysis methods are discussed. The effects of truncation in the Laplace and Fourier transform data analysis methods are described in detail. Methods for eliminating truncation errors from measured damping are presented. Implications of truncation effects in fast Fourier transform analysis are discussed. Limited comparison with test data is presented.

5

INTRODUCTION

Flight flutter testing is generally a time-consuming procedure. It involves the installation of complex excitation generators such as vanes, inertia exciters, or impulsive devices (ref. 1) as well as the response transducers and the associated electronic equipment. During flight testing, many flights are required to fully explore the aircraft critical flight spectrum, producing a large amount of test data which must be subsequently analyzed.

Considerable simplification in equipment installation may be obtained if turbulence excitation can be used instead of mechanical excitation. In any event, atmospheric turbulence and buffet degrade the response data from all types of mechanical excitation, except for random excitation, where it would most probably help more than hinder (ref. 2). Thus, the availability of suitable random response analysis methods, in addition to the existing harmonic analysis methods, would be a great advantage. The random analysis methods, like the current harmonic analysis methods, place the burden of data reduction on the computer, which, when used in the interactive mode with the test engineer, can provide a basis for real-time flutter testing.

The exciter installation and data acquisition and analysis problems are further compounded in space shuttle type vehicles, where weight is of paramount importance and the cost of exploring the entire critical flight spectrum with many flights prohibitive. The nonstationary nature of the flight environment and the relatively short duration of each flight within the atmosphere place a premium on the need for transmitting as much response data as possible,

and as quickly as possible, to the ground station. An increase either in the rate of sampling of the transducers, or in the number of transducers, is possible, if the data sample length can be reduced without a loss in the accuracy of the analysis.

A reduction in the sample length of the random response data is accompanied by a reduction in the statistical accuracy of the frequency domain modal response spectra. The statistical accuracy can be restored at the expense of resolution through a corresponding increase in the effective analysis bandwidth. This increase in analysis bandwidth produces a truncation effect in the response spectra. The truncation effect can occur in the frequency domain modal analysis derived from the Fourier transform of not only the impulse response time history but also the cross- and auto-correlation functions of response due to random and impulse-type excitations.

The effect of truncation is studied by using a single-degree-of-freedom system. Existing frequency domain harmonic analysis methods are briefly discussed as an introduction to the truncation effect and to illustrate the format of the data presentation.

HARMONIC ANALYSIS

The simplest method for obtaining aircraft modal frequency and damping data is through stick pulse generated free decay data (figs. 1 and 2). However, narrow band filtering is required both to isolate each mode in turn and to minimize noise due to the presence of turbulence. Computerized least squares fit methods such as the Moving Block Analysis (ref. 3) can be used to obtain damping data from the log decrement of the decay once the resonant frequencies have been identified by spectral analysis.

Stick pulses, in general, may not excite all the modes of interest and may produce an unconservative estimate of the damping. For close resonances, narrow band filtering may not isolate each mode, resulting in a beating decay response (fig. 1). Under such circumstances, it is possible to extract meaningful data only if the modal damping and amplitudes are comparable in each of the modes. It is, however, possible, through the Fourier transform, to transform the decay data into the frequency domain (figs. 3 and 4) and thereby resolve the modes.

This Fourier transform process can be illustrated mathematically by considering the relationship between the response $y(t)$ of a linear system and a general force $x(t)$, given by

$$y(t) = \int_{-\infty}^{\infty} h(\tau)\, x\,(t-\tau)\, d\tau \qquad (1)$$

where $h(\tau)$ is the impulse response function of the system at time τ. For a single-degree-of-freedom system, the impulse response function is given by

$$h(\tau) = \frac{e^{-\delta\omega_r \tau}}{m\,\omega_r\sqrt{1-\delta^2}} \operatorname{Sin}\omega_r\sqrt{1-\delta^2}\;\tau \qquad (2)$$

where:

- m is the generalized mass,
- ω_r is the angular resonant frequency, and
- δ is the viscous damping coefficient.

If the force is of sufficiently short duration that it can be considered to be an impulse $I\delta(t)$, where $\delta(t)$ is the delta function, then the response time history reduces to

$$y(t) = h(t)\,I \qquad (3)$$

The response spectrum $y(i\omega)$, obtained from Fourier transform of the time history (eq. (1)), is related to the force spectrum $x(i\omega)$ by

$$y(i\omega) = H(i\omega)\,x(i\omega) \qquad (4)$$

where $H(i\omega)$ is the frequency response function of the system. For a single-degree-of-freedom system,

$$H(i\omega) = \frac{1}{m\,(\omega_r^2 - \omega^2 + 2i\delta\omega_r\omega)} \qquad (5)$$

The Fourier transforms of the response $y(t)$ and the force $x(t)$ are defined by

$$y(i\omega) = \frac{1}{2\pi}\int_{-\infty}^{\infty} y(t)\,e^{-i\omega t}dt \qquad (6)$$

and

$$x(i\omega) = \frac{1}{2\pi}\int_{-\infty}^{\infty} x(t)\,e^{-i\omega t}dt \qquad (7)$$

respectively. Again, if x(t) can be considered an impulse $I\delta(t)$, then the force spectrum reduces to

$$x(i\omega) = \frac{I}{2\pi} \tag{8}$$

and the response spectrum to

$$y(i\omega) = \frac{H(i\omega)\, I}{2\pi} \tag{9}$$

which is simply the system frequency response function multiplied by a constant.

Two formats can be used in the presentation of the frequency domain response data. In the response modulus vs frequency presentation (fig. 3), the resonant frequency is located approximately at the peak response, and the viscous damping coefficient, which is twice the structure damping, is obtained by dividing the half power point bandwidth by twice the resonant frequency.

It is accurate for well-separated modes. For close modes, as the modulus represents the total response vector from the origin and not necessarily the modal vector, errors in the measured modal frequency and the viscous damping coefficient may result. The extraction of modal damping may even be prevented by the failure to resolve the half power points (fig. 3).

To overcome these limitations, both amplitude and phase are retained and presented in a format of a Nyquist plot (fig. 4) in which the real part of the response is in phase and the imaginary part is out of phase relative to the excitation. This method of modal analysis was first suggested by Kennedy and Pancu (ref. 4). The resonant frequency is located at the point on the curve where the rate of change in arc length with frequency is at a maximum. The viscous damping coefficient is obtained from the half power points as previously described or by first measuring the angle ϕ subtended at the modal origin, by the arc between any frequency point f and the resonant frequency point f_r, and then using the relationship

$$\delta = \frac{f_r - f}{f_r} \operatorname{Cot}(\phi) \tag{10}$$

A strong feature of the Nyquist plot response data representation is that mode shapes can be identified by means of the modal response vector.

The more common method of generating the response Nyquist plots is by means of a slow sine sweep using mechanical in-flight excitation, such as inertia exciters, in which the force output is used as reference. This method has been computerized for multimodal analysis (ref. 5), employing a least

squares curve fit technique to minimize the effect of extraneous noise and used in a computer/test engineer interactive mode for flutter testing.

In transforming the free decay data as previously discussed, no truncation effects were observed due to the relatively high modal damping and the need for including one beat as a minimum in the decay sample. In the second example of a stick pulse excited decay (fig. 2), the decay was prematurely truncated after one and five seconds to illustrate the effect on the frequency domain response (fig. 5). The Nyquist plots of the response become more oval in appearance as the decay sample duration is progressively reduced. If the Nyquist plots are analyzed by the conventional method described above, unconservative estimates of the damping are obtained. (See table 1.) In order to obtain useful damping data from these Nyquist plots, a method eliminating the effect of truncation from the damping must first be developed.

TRUNCATION THEORY

Due to the similarity between the cross-correlation and the impulse-response functions with the auto-correlation function Ryy (τ) of a single-degree-of-freedom system excited by a constant spectrum force, S_p (ref. 2) and defined by

$$Ryy(\tau) = \frac{\pi S_p \, e^{-\delta\omega_r\tau}}{2m^2\omega_r{}^3\delta}\left(\text{Cos } \omega_r \sqrt{1-\delta^2}\,\tau + \frac{\delta}{\sqrt{1-\delta^2}} \text{ Sin } \omega_r \sqrt{1-\delta^2}\,\tau\right) \qquad (11)$$

it is only necessary to describe the equations for any one of the above functions. The impulse-response function and the cross-correlation function of a single-degree-of-freedom system, when excited by constant spectrum force, exist only for positive time.

If the Laplace transform or the single-sided Fourier transform of the autocorrelation function of the response Ryy (τ) is used, with limits of integration from zero to infinity, instead of the full Fourier transform, phase information is retained in the response spectrum (ref. 2). The resulting response spectrum $S(i\omega)$ is given by

$$S(i\omega) = \frac{S_p}{4m\omega_r{}^2\delta}\left(\frac{i\omega}{\omega_r} H(i\omega) + 2\delta H(i\omega)\right) \qquad (12)$$

The characteristic response function $\frac{S(i\omega)}{S_p}$ has properties similar to the frequency response function $H(i\omega)$. This method provides a powerful tool in

modal response analysis of random as well as impulse response data in the frequency domain. The previously described methods for extracting the modal damping and frequency can be employed as long as no truncation effect is present.

If we let $y(t)$ represent any of the above time functions, with the understanding that they exist only for positive time, the complex response spectrum $y(i\omega)$ is obtained from Fourier transform of $y(t)$.

$$y(i\omega) = \frac{1}{2\pi}\int_{-\infty}^{\infty} y(t)\, e^{-i\omega t}dt \qquad (13)$$

$$\text{where} \quad y(t) = 0 \quad \text{for} \quad t < 0$$

In reality, the response time history is truncated at some finite time τ_m. The resulting estimated response spectrum $\hat{y}(i\omega_1)$ (ref. 6) is given by the relationship

$$\hat{y}(i\omega_1) = \frac{1}{2\pi}\int_{0}^{\tau_m} y(t)\, e^{-i\omega_1 t}dt$$

$$= \frac{1}{2\pi}\int_{-\infty}^{\infty} D(t)\, y(t)\, e^{-i\omega_1 t}dt \qquad (14)$$

where $D(t)$ is the weighting or the truncation function.

Three weighting functions (ref. 7) are considered in this paper. They are the "do-nothing" or the boxcar weighting, generally defined by

$$D(t) = 1 \quad \text{for} \; -\tau_m < t < \tau_m$$
$$= 0 \quad \text{elsewhere} \qquad (15)$$

the Hanning weighting function defined by

$$D(t) = \frac{1}{2}\left(1 + \text{Cos}\,\frac{\pi t}{\tau_m}\right) \quad \text{for} \; -\tau_m < t < \tau_m$$
$$= 0 \quad \text{elsewhere} \qquad (16)$$

and the Bartlett weighting function defined by

$$D(t) = \left(1 - \frac{|t|}{\tau_m}\right) \quad \text{for} \; -\tau_m < t < \tau_m$$
$$= 0 \quad \text{elsewhere} \qquad (17)$$

The reverse Fourier transform for the response is given by

$$y(t) = \int_{-\infty}^{\infty} y(i\omega)\, e^{i\omega t} d\omega \tag{18}$$

On substituting for y(t) in equation (14) and rearranging the order of the integration, the estimate of the spectrum becomes

$$\begin{aligned} \hat{y}(i\omega) &= \frac{1}{2\pi} \int_{-\infty}^{\infty} \int_{0}^{\tau_m} D(t)\, e^{-i(\omega_1 - \omega)t}\, dt\, y(i\omega) d\omega \\ &= \int_{-\infty}^{\infty} Q(\omega_1 - \omega)\, y(i\omega)\, d\omega \end{aligned} \tag{19}$$

where

$$Q(\omega_1 - \omega) = \frac{1}{2\pi} \int_{0}^{\tau_m} D(t)\, e^{-i(\omega_1 - \omega)t} dt \tag{20}$$

$Q(\omega_1 - \omega)$ is referred to as the spectral window. The weighting functions defined by equations (16) to (18) and the corresponding spectral windows are illustrated in figure 6. In the application discussed in this paper, the spectral windows are complex (ref. 6 and 8) since the weighting functions are one sided and exist only in positive time from zero to τ_m.

TRUNCATED DATA REDUCTION

For a linear system excited by random force (or impulse) of constant spectral density, the response spectrum $y(i\omega)$ is proportional to the frequency response function of the system. Equation (19), with $y(i\omega)$ replaced by the frequency response function of a single-degree-of-freedom system and a constant force spectrum, has been integrated by using contour integration for the "do-nothing" and the Bartlett weighting in references 6 and 8, respectively. It has recently been solved by the author for the Hanning weighting. A typical effect of the truncation due to the Hanning weighting is illustrated in figure 7. The single-degree-of-freedom response plots have been normalized relative to the untruncated plot. The other two weighting functions differ only in the degree of truncation effect. The "do-nothing" weighting function, while exhibiting the smallest truncation effect, suffers from the undesirable side lobes (fig. 5) which may be mistaken for modes or may interfere with other nearby modes. The Bartlett weighting function suffers a greater resolution loss, as can be seen by comparing figure 8 with figure 5.

The resonant frequency is still identified by the peak rate of change of arc length with frequency, but the procedure for estimating the damping from the truncated curves is different from the methods previously described. At

first (ref. 6 and 8), the damping coefficient was extracted with the assistance of a nondimensional parameter defined by the peak rate of change of arc length with frequency, divided by the radius of curvature at the resonant frequency, from theoretically predicted curves. In these curves, the above parameter is plotted as a function of the resonant frequency multiplied by the true damping coefficient. These curves were originally developed for use in high frequency structural response studies and consequently are unsuitable for flutter data analysis due to the relatively low aircraft response frequencies.

A more useful graphical format, which provides direct damping readout, is presented in this paper and illustrated in figure 9 for the Hanning truncation. The measured damping coefficient δ^* is plotted against the true damping coefficient δ as a function of the ratio of the effective data analysis bandwidth Δf divided by the resonant frequency. The effective analysis bandwidth Δf is related to the maximum truncation time τ_m by

$$\Delta f = \frac{1}{2\tau_m} \tag{21}$$

The measured damping coefficient δ^* is defined by

$$\delta^* = \frac{2\rho}{ds}\left(\frac{df}{f_r}\right) \tag{22}$$

where ρ is the radius of curvature at resonance, and

ds is the arc length at resonance contained within the frequency interval of df

It can be observed that as the maximum truncation time becomes large, the measured viscous damping coefficient approaches the true value.

This method of obtaining the damping from the truncation-affected single-degree-of-freedom system Nyquist plots has been computerized for potential use in real-time analysis. The number of iterations required to converge to the correct damping from the estimated damping is illustrated in figure 10. The convergence is carried out in two or three sequences and is very rapid. The number of steps in the initial sequence is selected to speed up the iteration, especially in cases of severe truncation.

The damping of the free decay record (fig. 2) as obtained by the computerized method for the "do-nothing", Hanning, and Bartlett truncations, a least squares fit to the free decay, and the restored Nyquist plot method (fig. 11) are summarized in table 2. The method of restoring the Nyquist (ref. 9) plot involves the weighting of the decay with a known exponential weighting to meet the required 55 dB dynamic range criteria (ref. 10) for the decay. Analysis is thereafter carried out conventionally and the damping

corresponding to the exponential weighting is subtracted from the measured damping to arrive at the true modal damping. It is more common to apply the exponential weighting function to the correlation function. This method has been used in flight flutter testing in England (ref. 11). The results from the analysis of the one-second decay record indicate the existence of a lower bound on the accuracy for the above frequency domain analysis methods.

TRUNCATION IN POWER SPECTRAL DENSITY

A method based on the cross-spectral analysis previously discussed was developed to predict the truncation effect in power spectral density (PSD) analysis. The effect of the truncation on the normalized PSD is illustrated in figure 12 for the Hanning weighting. A computer program was developed to obtain the damping from the 3 dB points by using the quadratic curve fit. A graphical method for obtaining the true damping coefficient δ from the measured damping coefficient $\hat{\delta}$ for various ratios of effective analysis bandwidth to resonant frequency is illustrated in figure 13.

A Hanning smoothed power spectral density plot of a typical aircraft response to high-speed buffet is illustrated in figure 14. Due to the very high speed, no reliable flutter test data are available for comparison. The analysis bandwidth of 0.5 Hz produces a truncation error in the two predominant modes at 10.2 Hz and 14.6 Hz. On allowing for the truncation effect, the viscous damping coefficients from the measured 3 dB point values of 0.11 and 0.044 are reduced to 0.068 and 0.02 for the two frequencies, respectively. This method suffers from the same inaccuracies as the modulus method previously discussed. It does, however, provide an indication of the damping where none previously existed.

FAST FOURIER TRANSFORM AND TRUNCATION

The above methods have been basically developed for the Blackman and Tuckey type of analysis (ref. 7). Truncation effects occur also in the fast Fourier transform (FFT) method of analysis. An indication as to the type of truncation present in FFT analysis of cross spectra is obtained from reference 12. The expected cross-spectral estimate $E\left[Sxy(f,T,k)\right]$ is given by

$$E\left[Sxy(f,T,k)\right] = \frac{1}{2\pi}\int_{-T}^{T}\left(1 - \frac{|\tau|}{\tau_m}\right) Rxy(\tau)\, e^{-i\omega\tau} d\tau \qquad (23)$$

As the cross-correlation function of a single-degree-of-freedom system excited by white noise is one sided, as previously discussed, it is concluded that the estimated cross spectrum obtained from FFT analysis is subject to Bartlett truncation errors.

The effect of truncation on the normalized PSD and cross spectral peak response is illustrated in figure 15 as a function of the resonant frequency multiplied by the maximum time delay and the viscous damping coefficient, $f_r \tau_m \delta$. It is observed that for the "do-nothing" truncation, the curve reaches unity near $f_r \tau_m \delta = 1$. This corresponds not only to the damping criteria for cross-spectral analysis established in reference 9, but also to the rule of thumb for PSD resolution for the analysis bandwidth to be one-fourth of the 3 dB point response bandwidth.

Attention is drawn to the fact that the Bartlett truncation curve converges to unity very slowly. Thus the use of cross-correlation functions obtained from the indirect method of first computing the spectra using the FFT and then transforming to time domain, will not only have the Bartlett truncation error but also an additional truncation error in transforming from the frequency domain to the time domain. These truncation errors in correlation functions are discussed in references 13, 14 and 15. Thus a very large number of transformation points must be used in determining the correlation function through the indirect method.

CONCLUSION

Methods for eliminating truncation errors from modal frequency and damping data have been presented for the cross- and power-spectral analysis. These methods have the potential for use in a computer/test engineer interactive mode, for random and impulsive-type response data analysis. Future work will include an evaluation of the methods against simulated and real flutter test data with buffet and turbulence excitation and the study of truncation effects in FFT-type analysis involving multiple Fourier transform operations.

REFERENCES

1. Baird, E. F., and Clark, W. B.: Recent Developments in Flight Flutter Testing in the United States. AGARD Report No. 596, Dec. 1972.

2. Kandianis, F.: Frequency Response of Structures and the Effects of Noise on its Estimates from the Transient Response. J. Sound Vib. 15(2), 1971.

3. Hurley, S. R.: The Application of Digital Computers to Near-Real-Time Processing of Flutter Test Data. NASA Symposium of Flutter Testing Techniques, Oct. 1975. (Paper No. of this compilation)

4. Kennedy, C. C., and Pancu, C.D.P.: Use of Vectors in Vibration Measurement and Analysis. J. Aero. Sci., 1947.

5. Gaukroger, D. R., Skingle, C. W. and Heron, K. H.: Numerical Analysis of Vector Response Loci. J. Sound Vib. 29(3), 1973.

6. Clarkson, B. L., and Mercer, C. A.: Use of Cross Correlation in Studying the Response of Lightly Damped Structures to Random Forces, AIAA J. 3, 1965.

7. Blackman, R. B., and Tukey, J. W.: Measurement of Power Spectra. Dover Publications, 1959.

8. Soovere, J., and Clarkson, B. L.: Frequency Response Function from Cross Correlation: Bartlett Weighting Function. AIAA J. 5, 1967.

9. White, R. G.: Evaluation of the Dynamic Characteristics of Structures by Transient Testing. J. Sound Vib. 15, 1971.

10. White, R. G.: Use of Transient Excitation in the Dynamic Analysis of Structures. R. Ae. S. J. 73, 1969.

11. Baldock, J. C. A., and Skingle, C. W.: Flutter Technology in the United Kingdom. AIAA Dynamics Specialist Conference, Williamsburg, 1973.

12. Bendat, J. S., and Piersol, A. G.: Random Data: Analysis and Measurement Procedures. Wiley-Interscience, 1971.

13. Mercer, C. A.: Note on Digital Estimation of Correlation Functions. J. Sound Vib. 27(2), 1973.

14. Holmes, P. J.: On the Practical Estimation of Spectra and Correlation Functions of Transient Signals. J. Sound Vib. 32(4), 1974.

15. Brownlee, L. R.: Comment on "Note on Digital Estimation of Correlation Functions." J. Sound Vib. 32(4), 1974.

TABLE 1. VISCOUS DAMPING COEFFICIENT OF TRUNCATED PLOTS DETERMINED BY USING EQUATION (10).

Decay Time, Seconds	"Do-Nothing" Truncation	Hanning Truncation	Bartlett Truncation
1	0.186	0.336	0.248
5	0.048	0.073	0.068

TABLE 2. COMPARISON OF VISCOUS DAMPING COEFFICIENT BY VARIOUS METHODS.

Decay Time, Seconds	Least Square Decay	Restored Nyquist Plot	TRUNCATION THEORY		
			"Do-Nothing"	Hanning	Bartlett
1	0.045	0.092	0.037	-	0.035-0.059
5	0.038	0.040	0.030	0.037	0.044

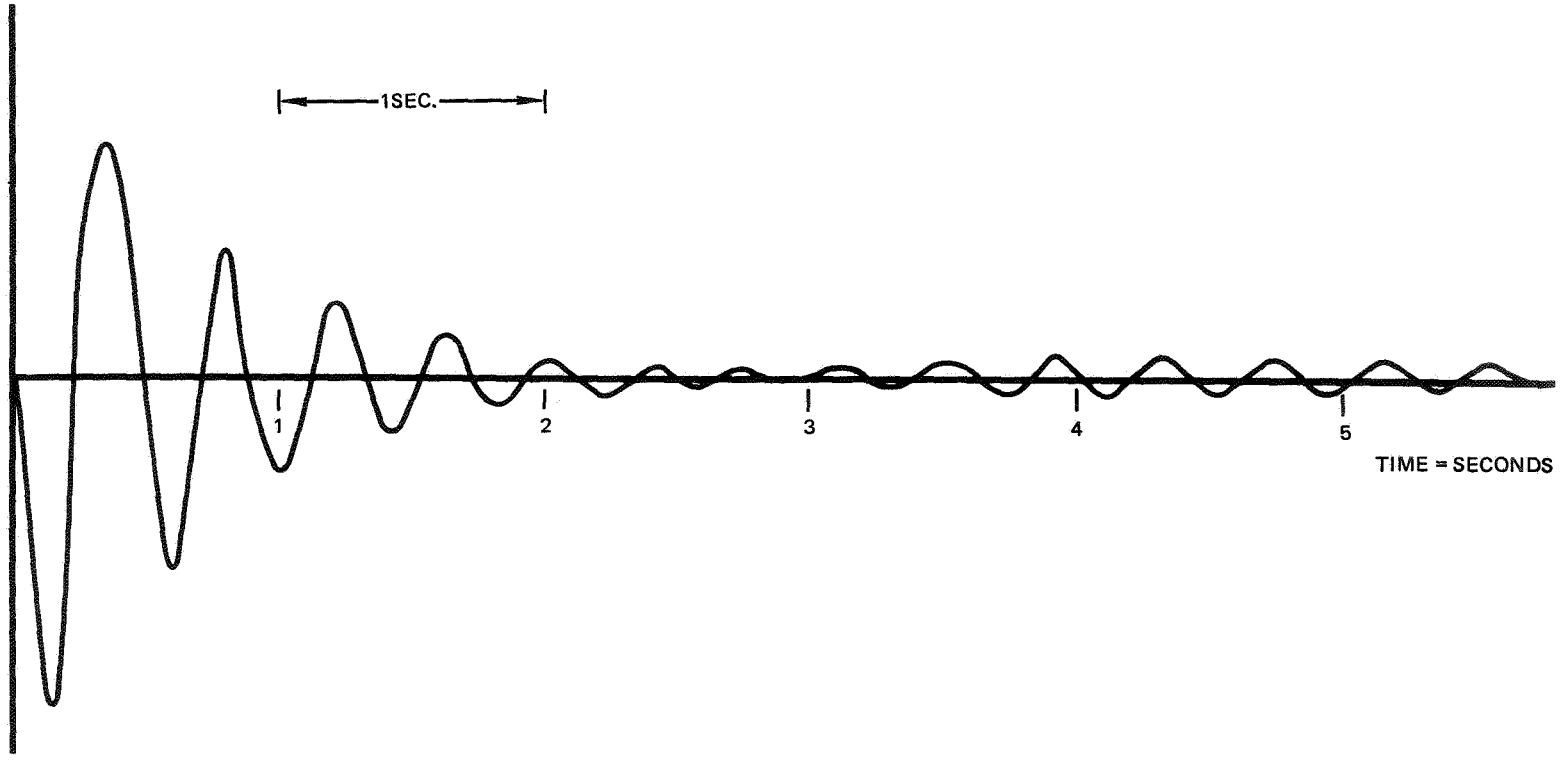

Figure 1. Typical Filtered Stick Pulse Excited Delay with Beating.

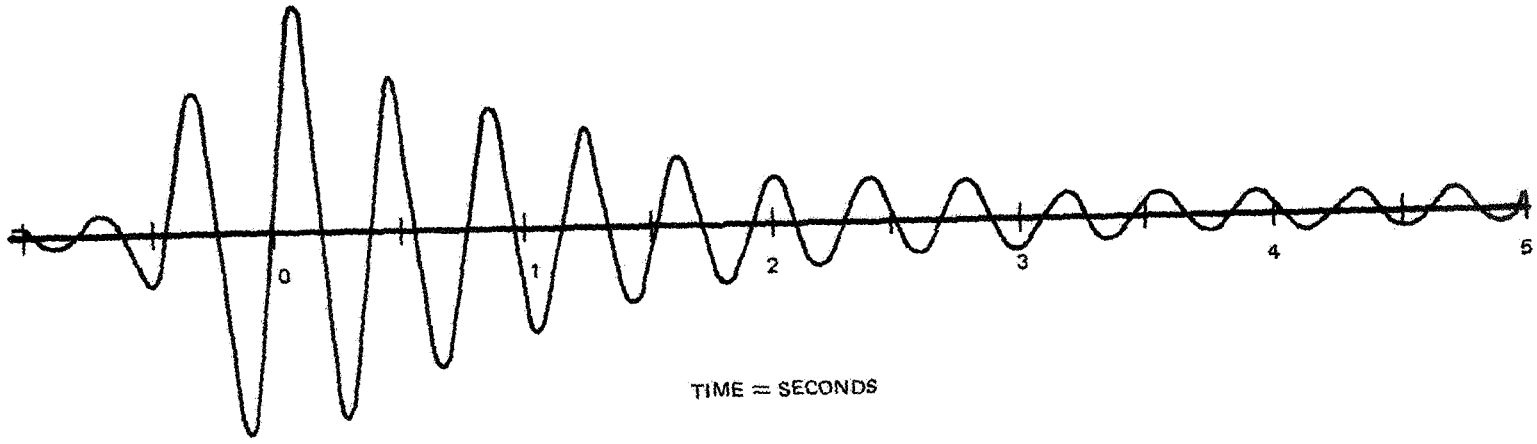

Figure 2. Typical Filtered Single Mode Stick Pulse Excited Decay.

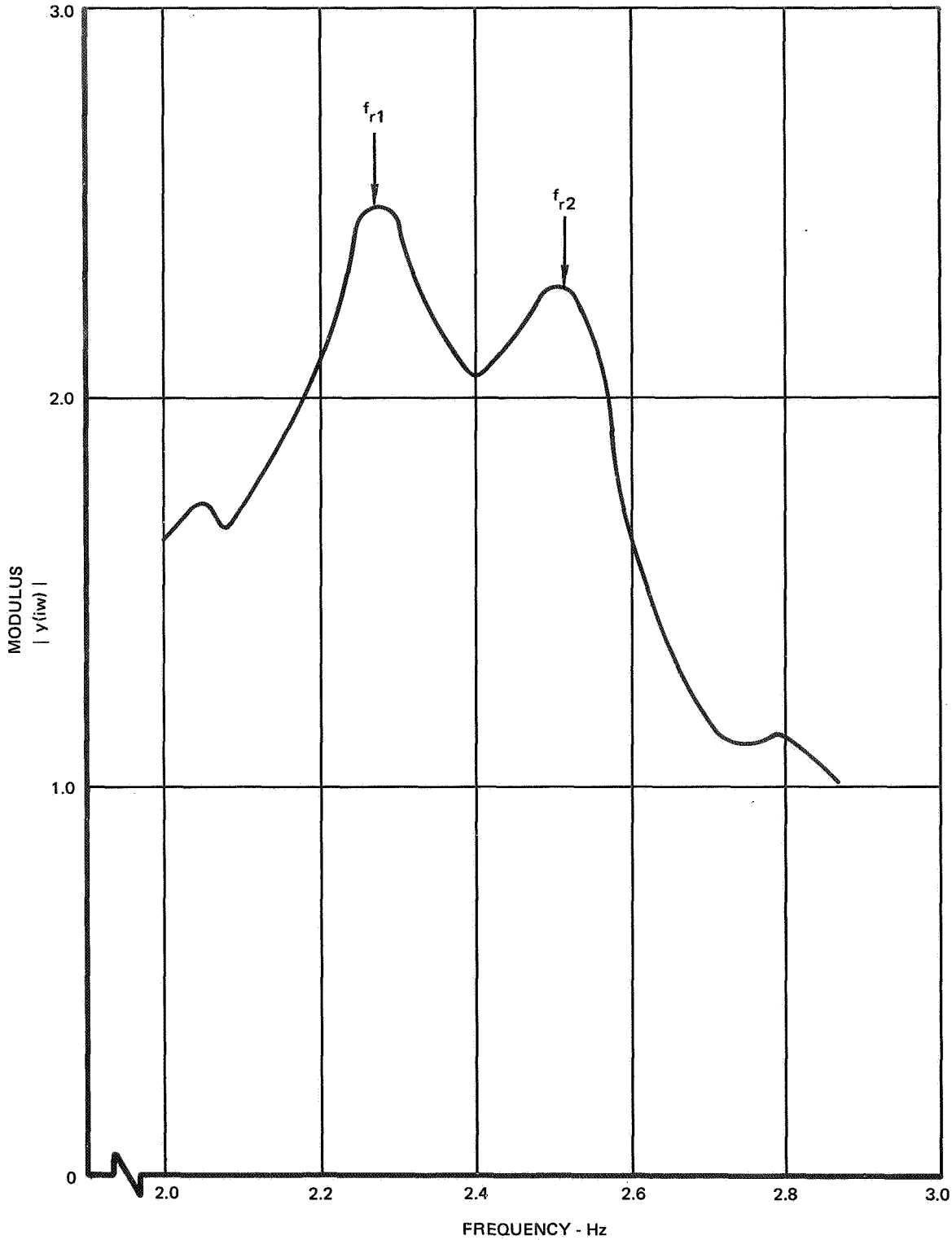

Figure 3. Modulus of the Fourier Transform of Beating Stick Pulse Excited Decay.

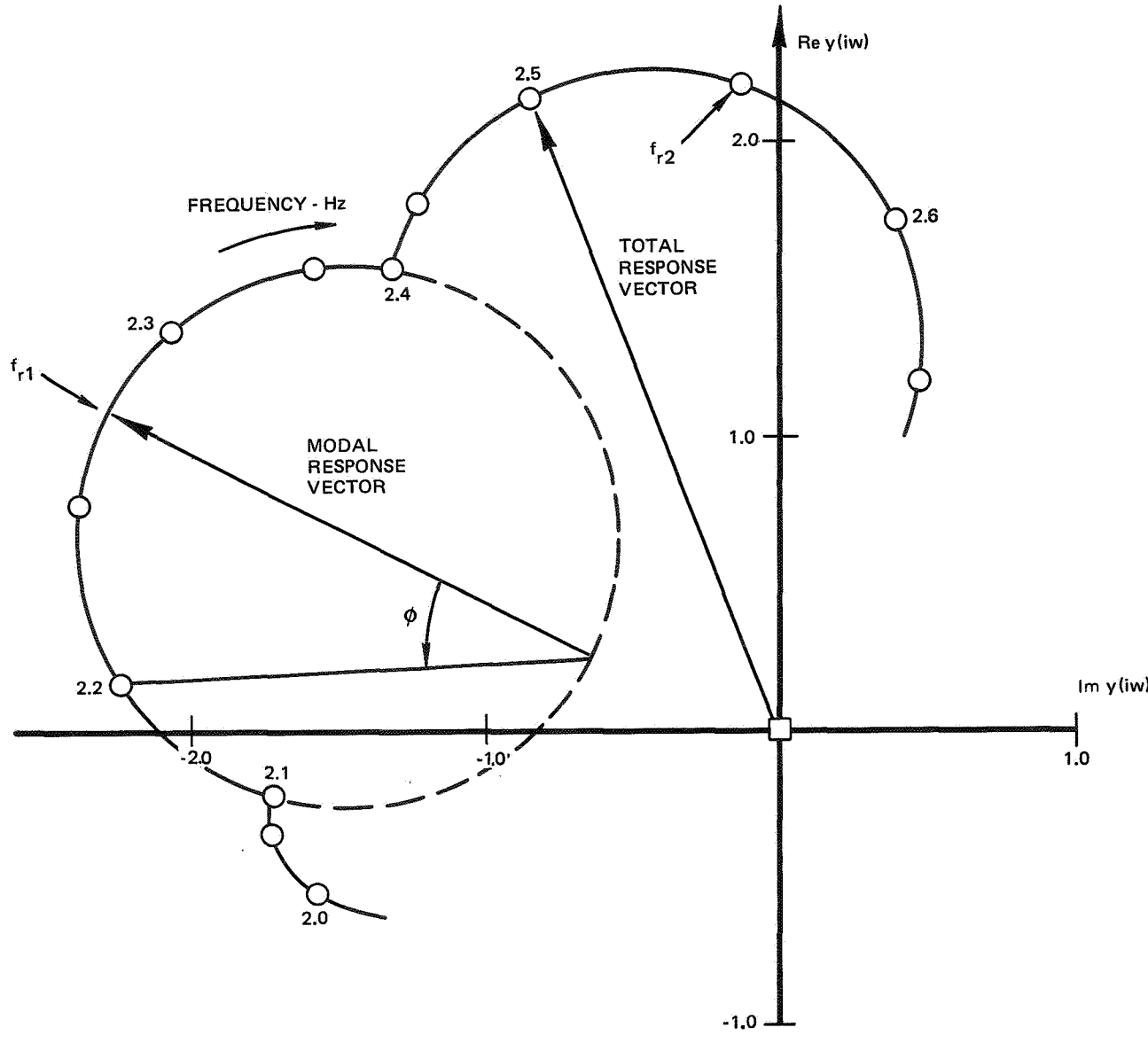

Figure 4. Fourier Transform of Beating Stick Pulse Excited Decay.

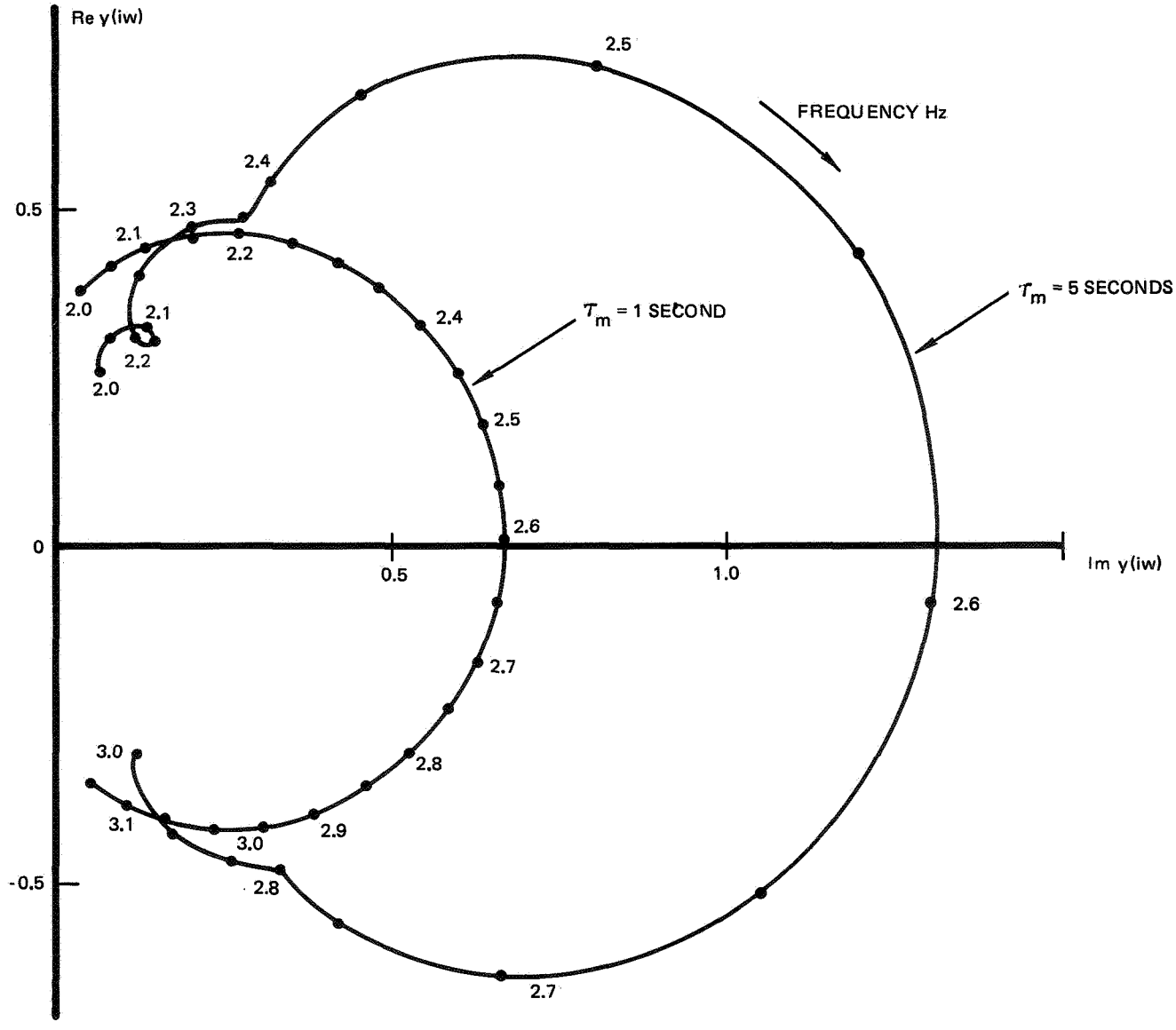

Figure 5. Fourier Transform of Stick Pulse Excited Single Mode Decay Showing Truncation Effect.

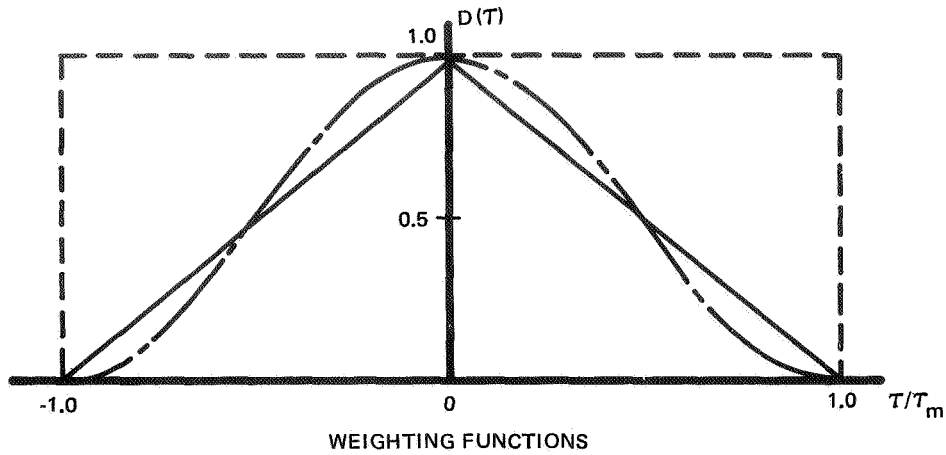

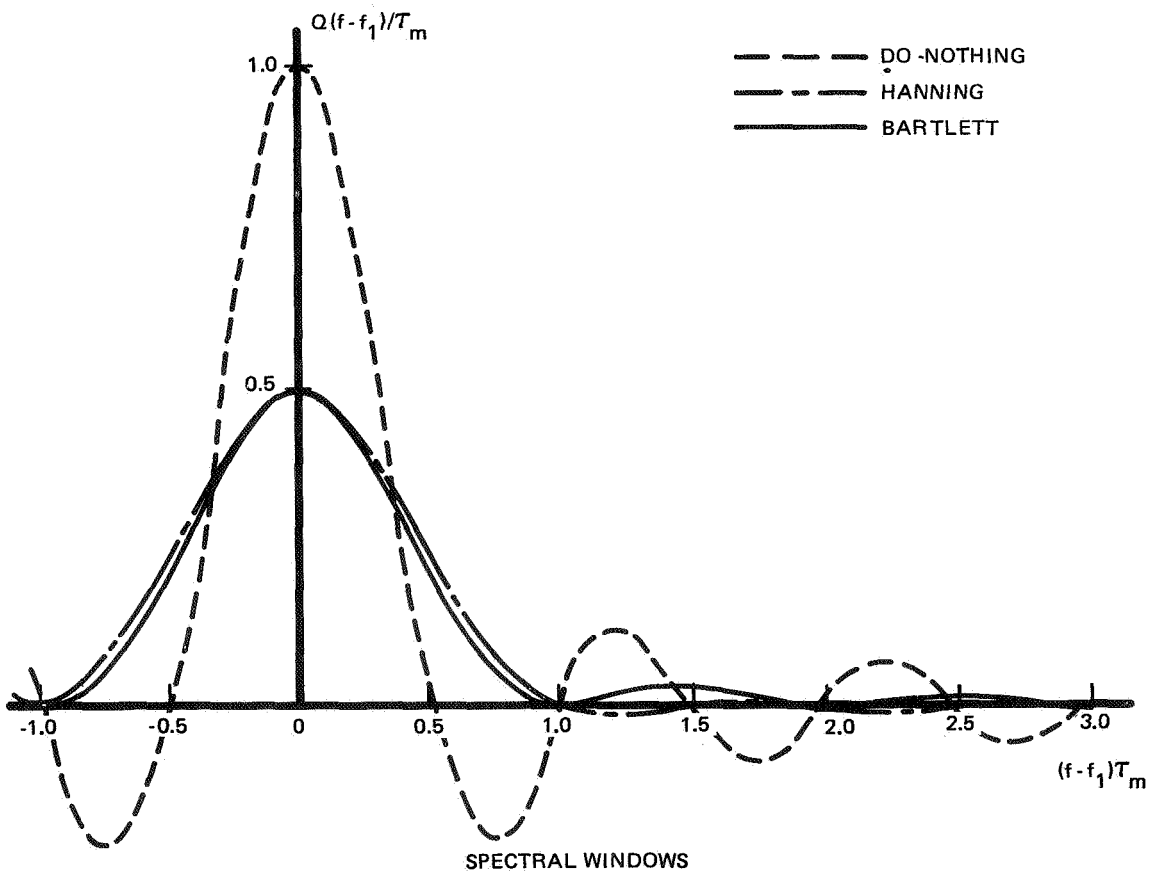

Figure 6. Spectral Windows and Weighting Functions.

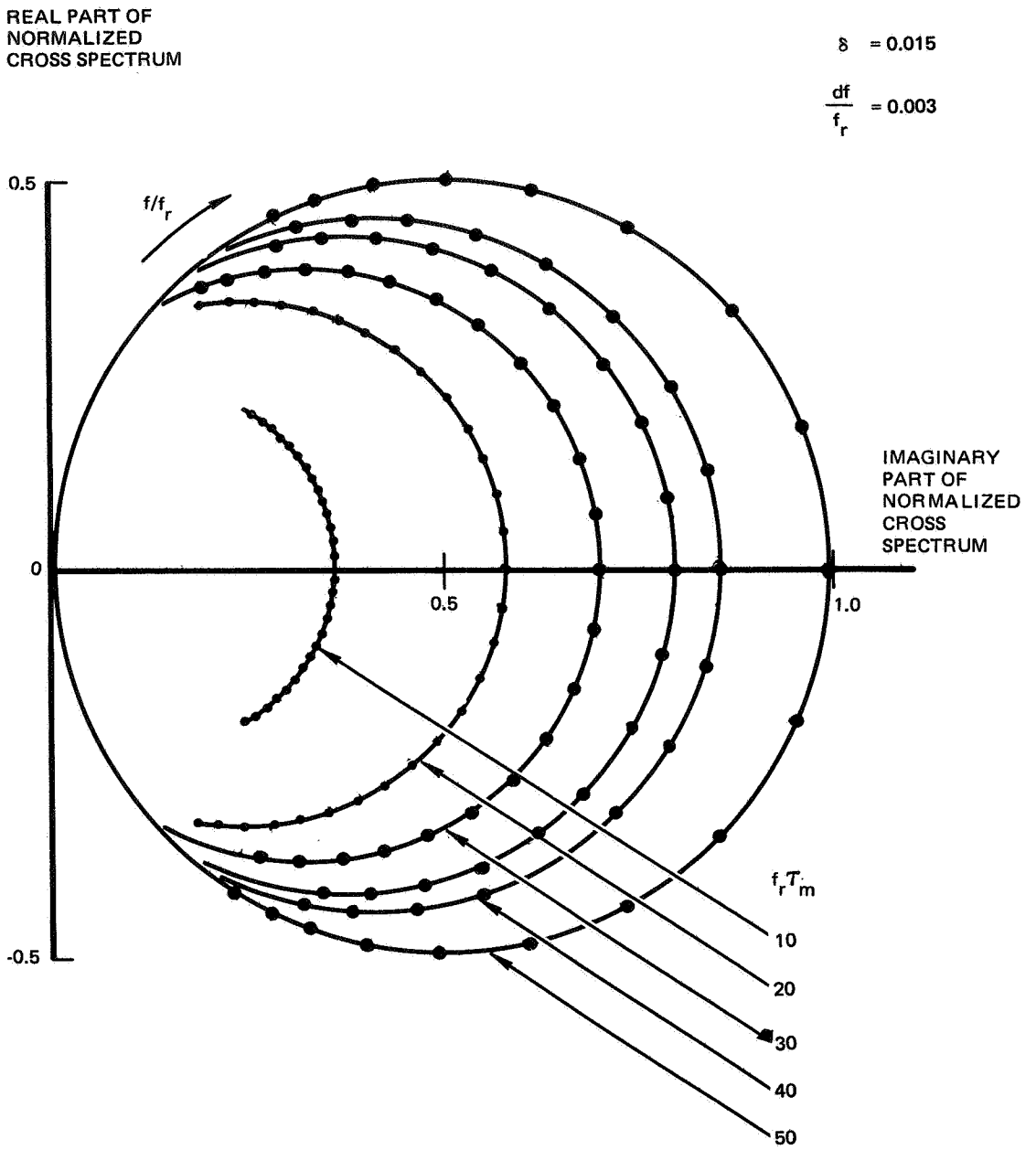

Figure 7. The Effect of Truncation on the Normalized Cross Spectrum of a Single-Degree-of-Freedom System Excited by White Noise - Hanning Weighting.

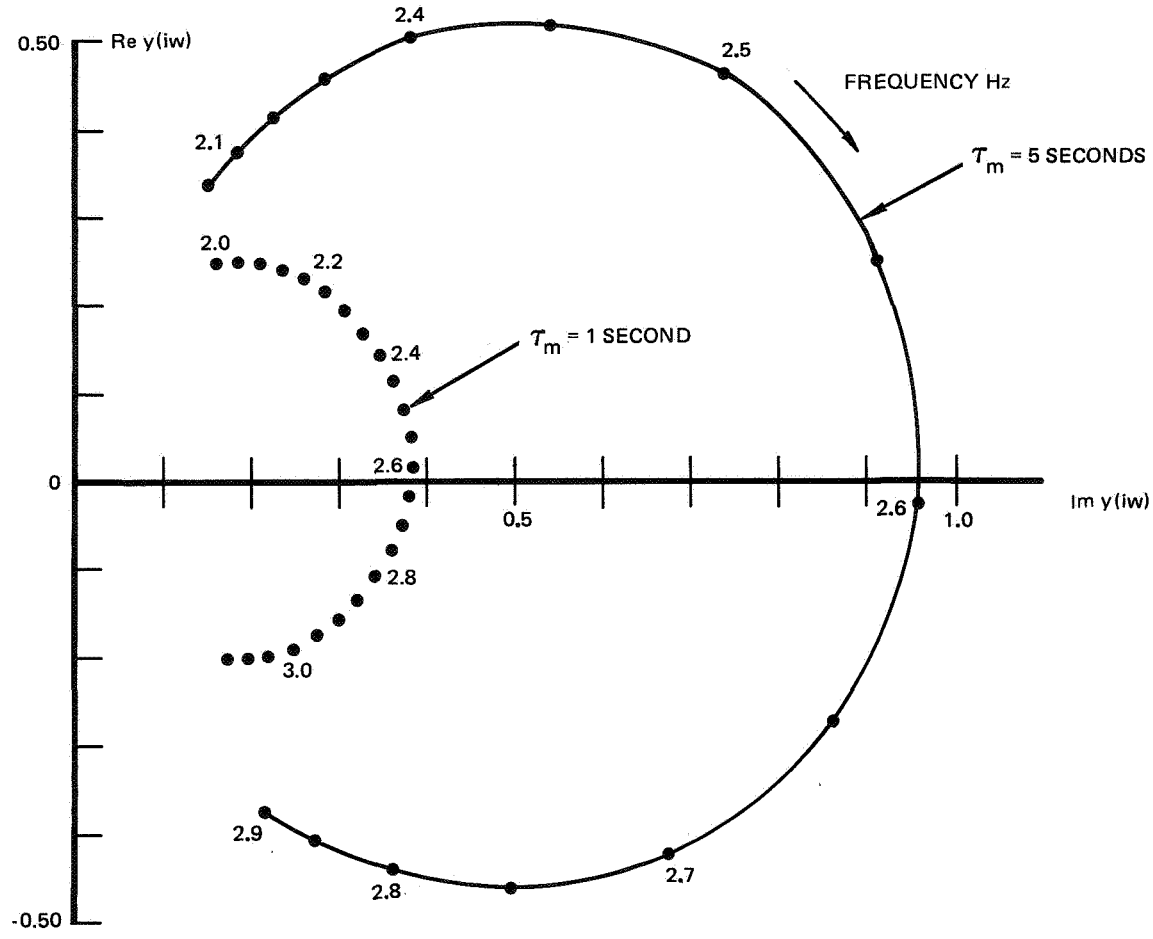

Figure 8. Fourier Transform of Stick Pulse Excited Decay with Bartlett Weighting.

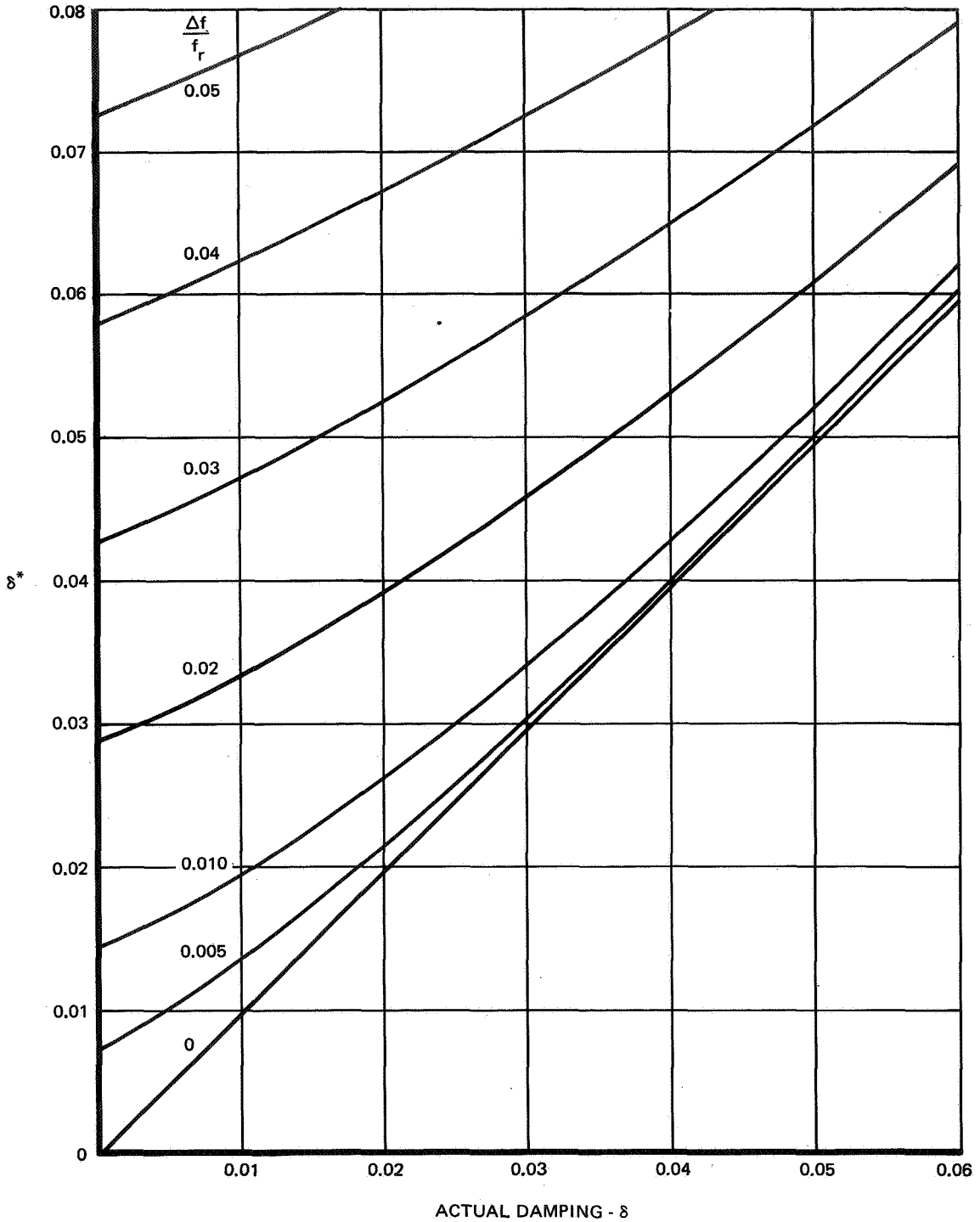

Figure 9. Method for Obtaining Damping from Truncation Affected Cross Spectra of a Single-Degree-of-Freedom System - Hanning Weighting.

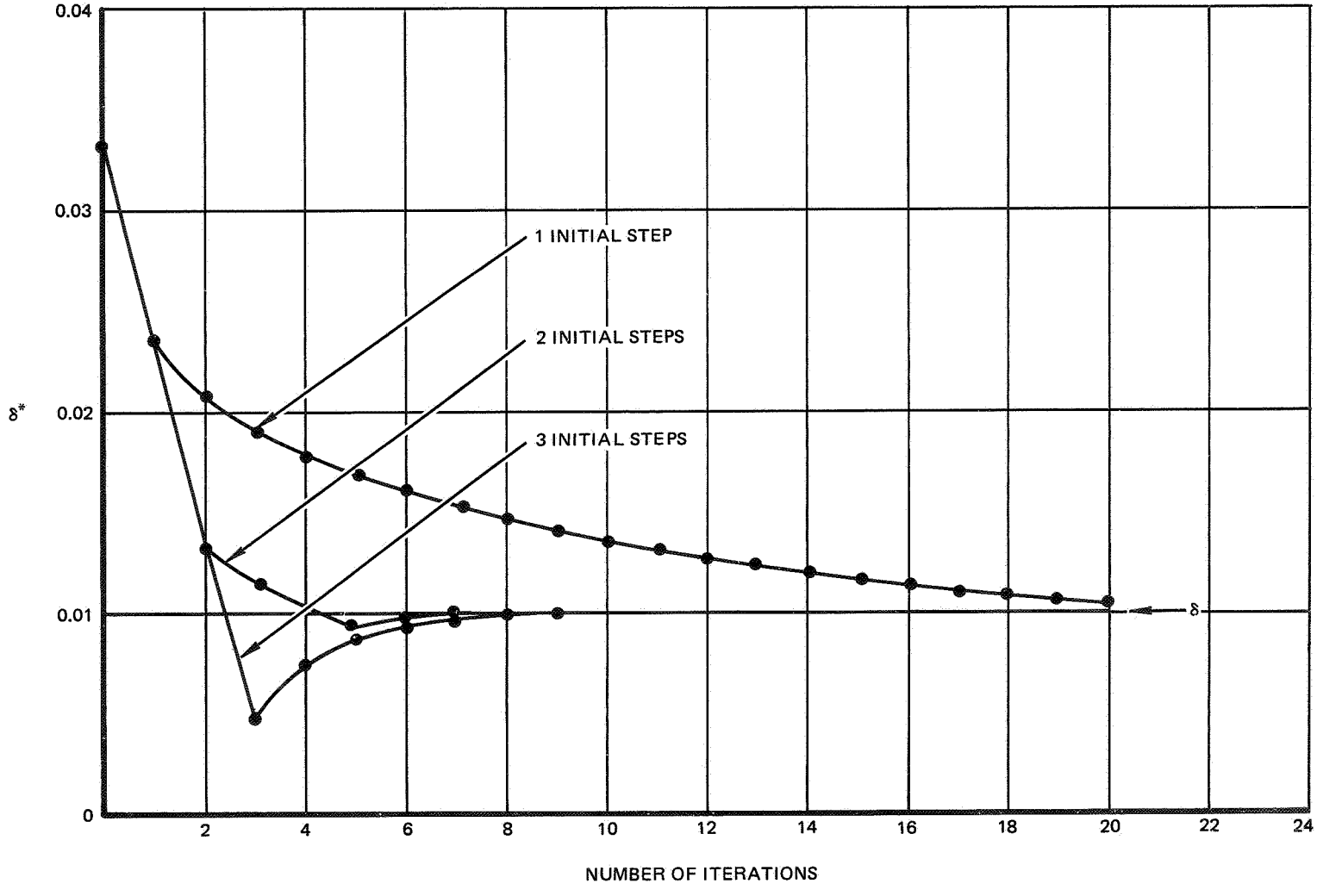

Figure 10. Typical Iteration Patterns - Hanning Truncation.

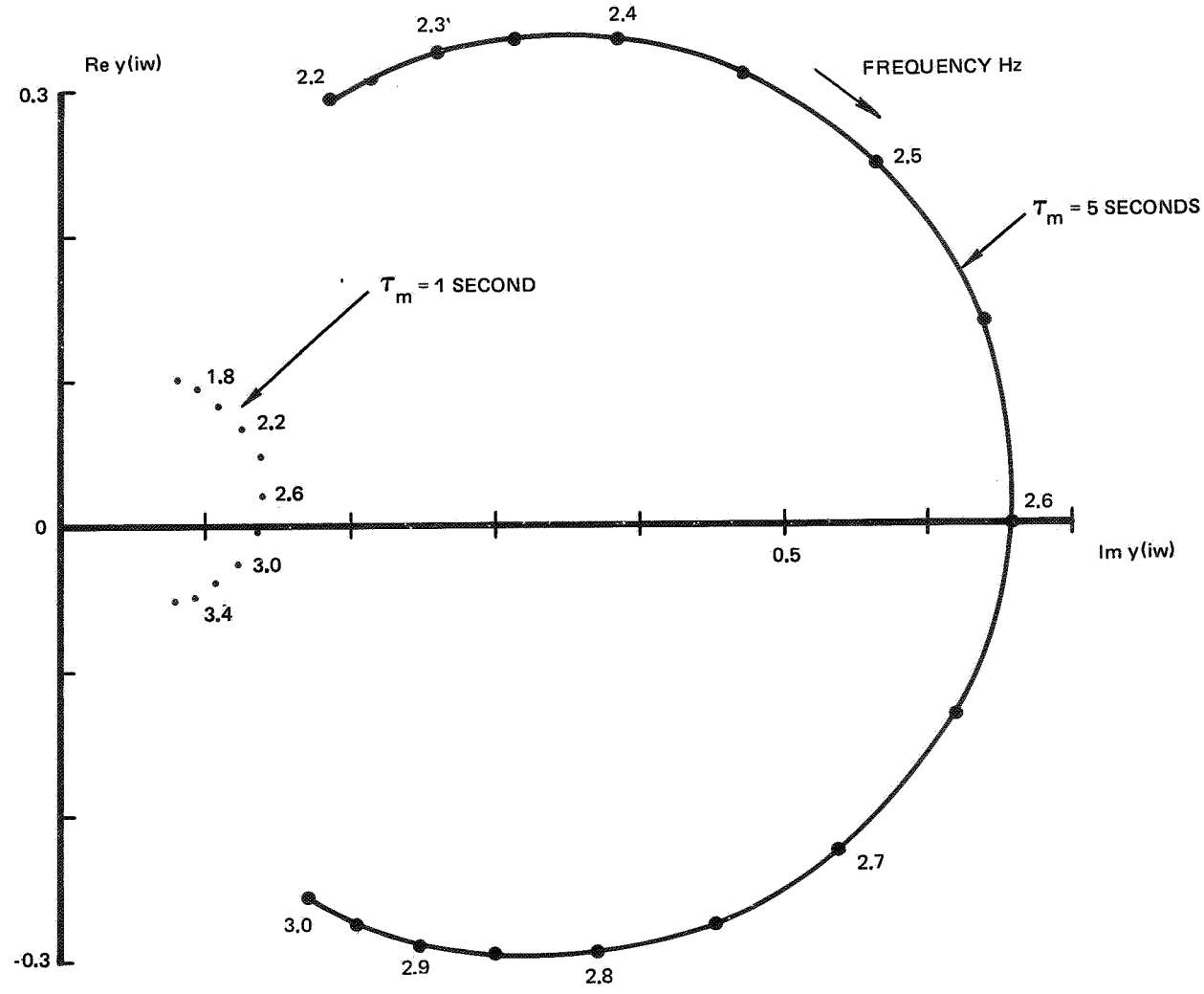

Figure 11. Restored Fourier Transform of Stick Pulse Excited Single Mode Decay Using Exponential Weighting Function.

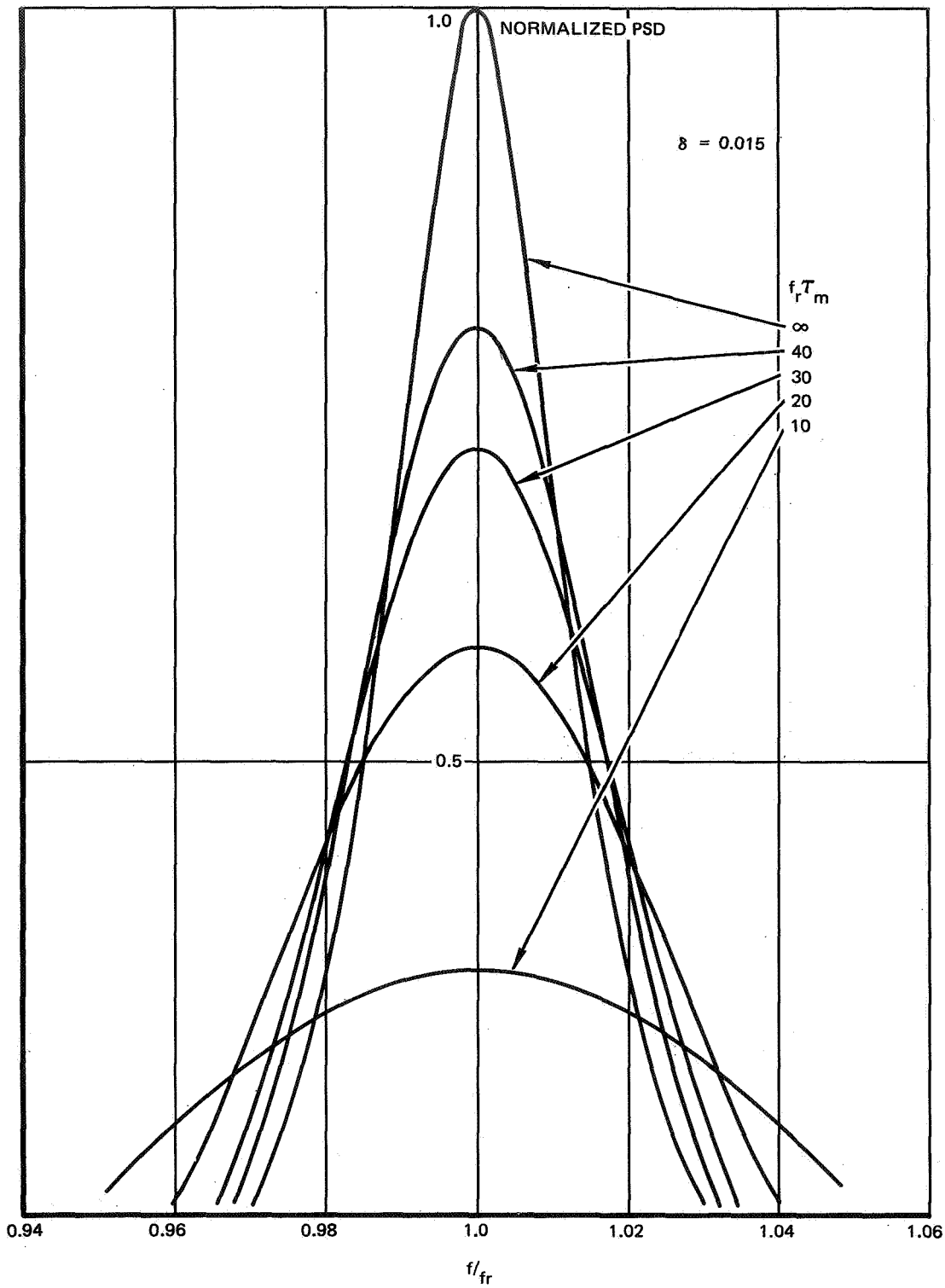

Figure 12. The Effect of Truncation on the Normalized PSD of a Single-Degree-of-Freedom System Excited by White Noise - Hanning Weighting Function.

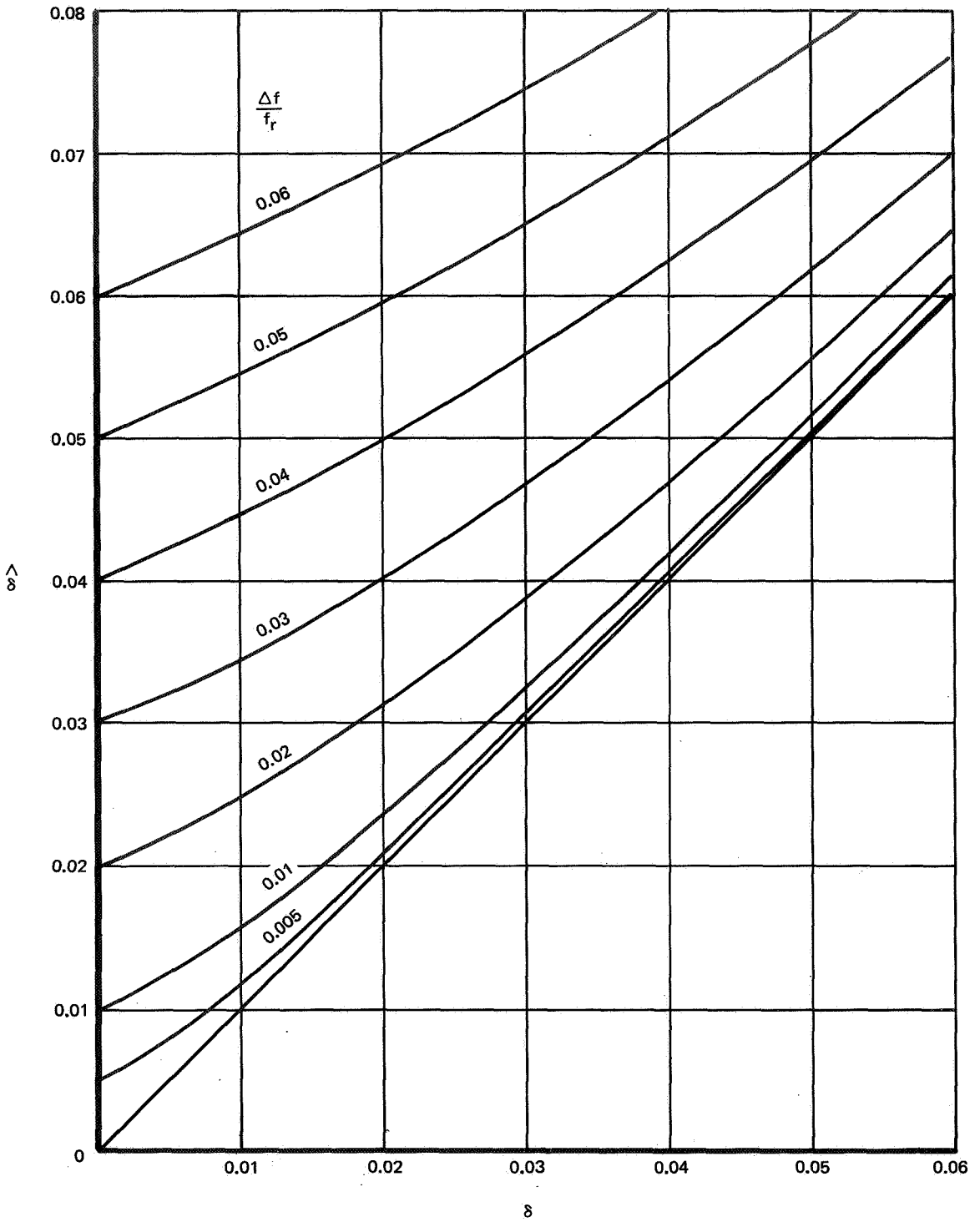

Figure 13. Correction to 3 dB Point Measured Damping from Single-Degree-of-Freedom System Response PSD - Hanning Weighting.

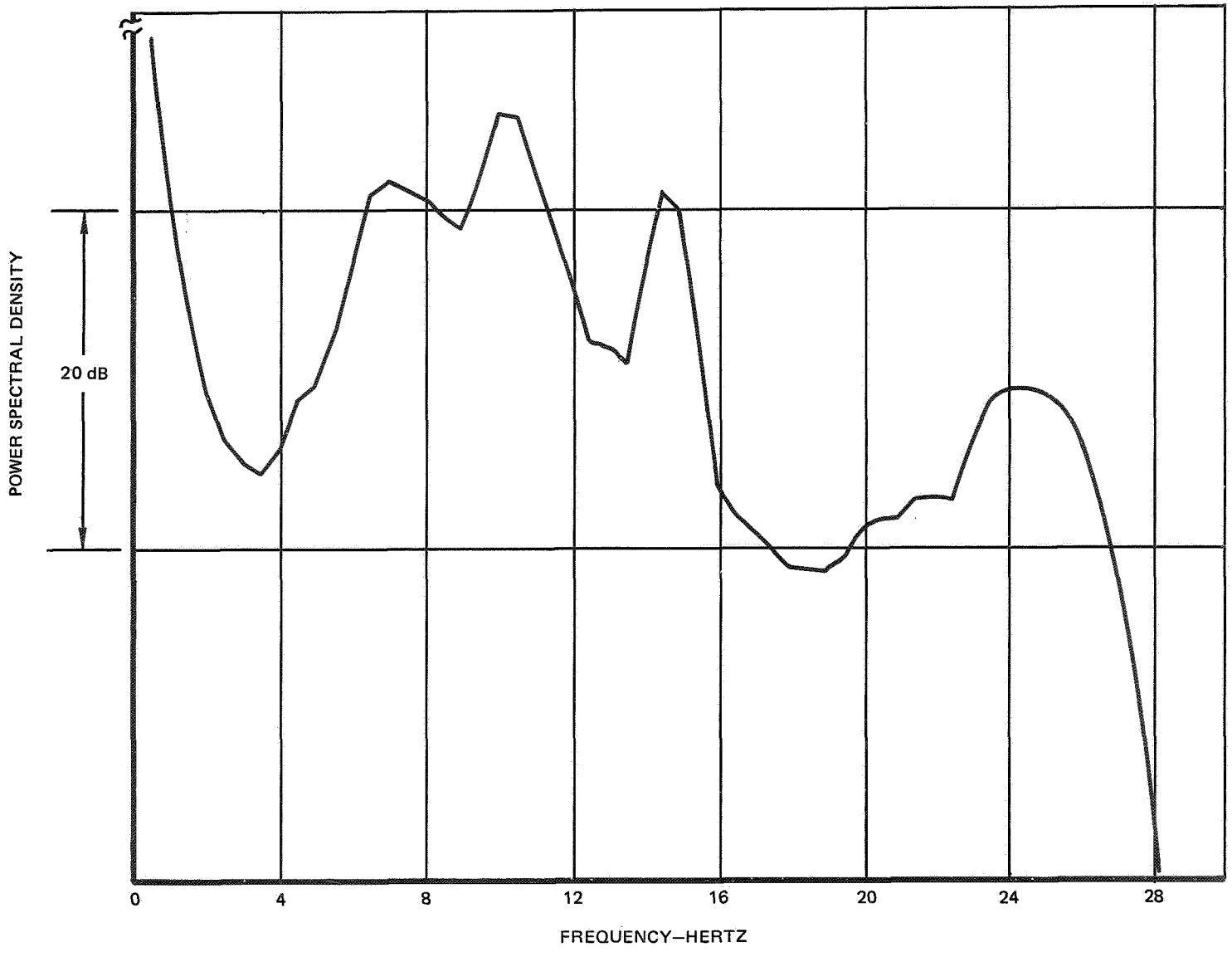

Figure 14. Typical Response Spectrum for Aircraft Excited by High-Speed Buffet.

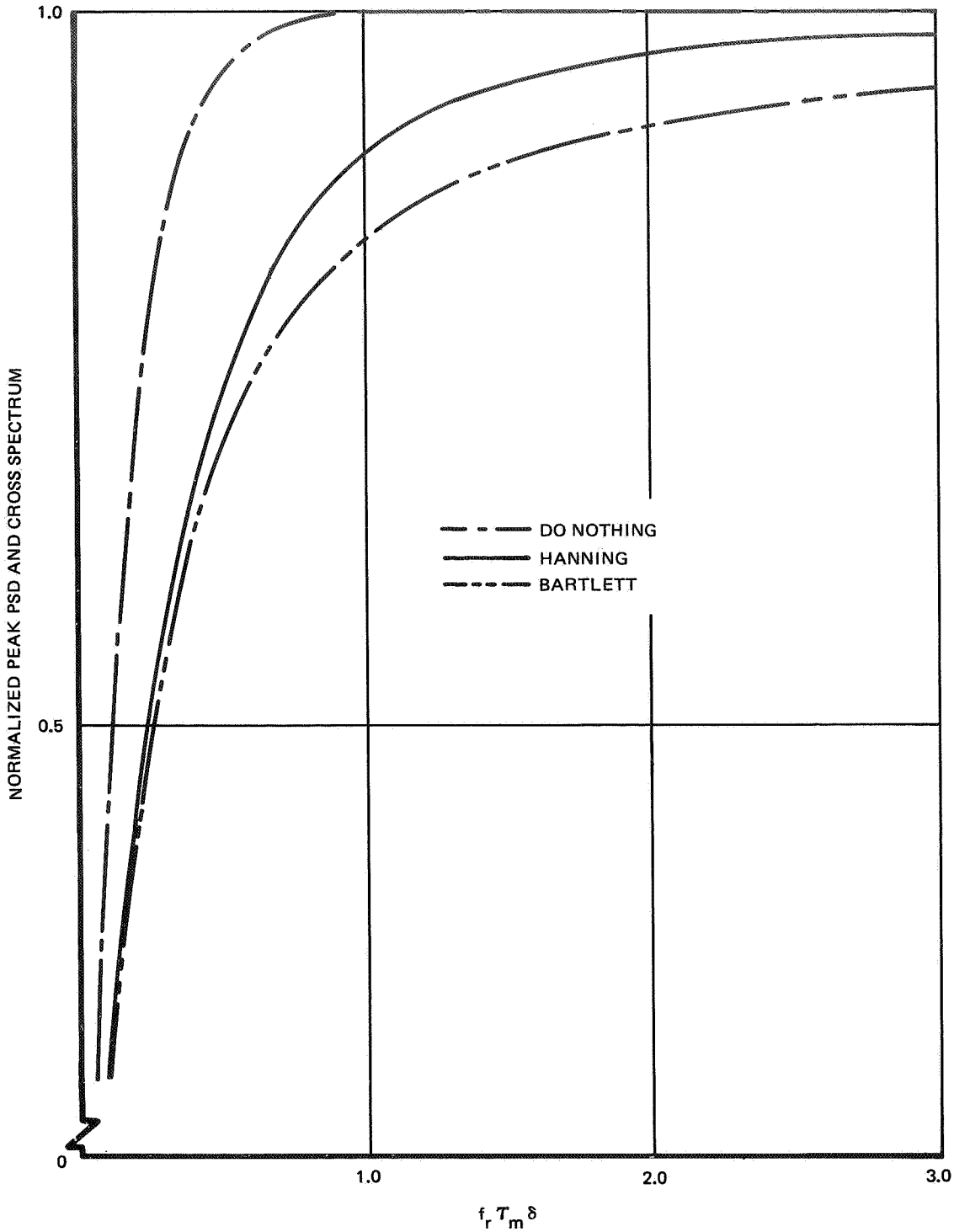

Figure 15. Effect of Truncation on the Peak PSD and Cross Spectral Response Resolution of a Single-Degree-of-Freedom System Excited by White Noise.